DALTON
FULL PAPER

# Electronic structure of Mo and W $[M_7O_{24}]^{6-}$ isopolyanions

**Adam J. Bridgeman** *[a] **and Germán Cavigliasso** [a,b]

[a] *Department of Chemistry, University of Hull, Kingston upon Hull, UK HU6 7RX. E-mail: A.J.Bridgeman@hull.ac.uk*
[b] *Department of Chemistry, University of Cambridge, Lensfield Road, Cambridge, UK CB2 1EW*

***Received 10th December 2001, Accepted 19th February 2002***
***First published as an Advance Article on the web 19th April 2002***

The structure and bonding in $[M_7O_{24}]^{6-}$ isopolyanions of Mo and W have been investigated using density-functional methods. Good computational–experimental agreement for the geometrical parameters has been obtained. The electronic structure of the anions has been probed with molecular-orbital and Mulliken–Mayer methods. All M–O interactions have been found to be largely M d–O p in character. Multicentred σ and π bonding involving different metal and bridging-oxygen atoms has been observed, and some of the corresponding molecular orbitals can be described in terms of $[M_nO_n]$ closed loops. Mayer indexes correspond to fractional multiple character for terminal bonds, and approximately single or low-order character for bridging bonds, and are thus in satisfactory agreement with bond-valence results. The valency analysis has yielded similar overall bonding capacity for the various oxygen atoms. A distribution of the negative charge over all types of oxygen sites, and metal charges considerably smaller than the formal oxidation states have been obtained from the Mulliken analysis.

## Introduction

Polyoxometalates constitute an immense class of compounds in number and diversity,[1,2] and exhibit remarkable chemical and physical properties, their actual and potential applications spanning a variety of fields, including medicine, catalysis, solid-state technology, and chemical analysis.[2–4] The formation of polymeric oxoanions is, in general, a phenomenon largely limited to the early transition metals in groups 5 and 6, and in particular to molybdenum and tungsten, which have been considered the "polyoxoanion formers par excellence".[2]

Most of the typical polyanion structures exhibit interpenetrating closed loops, formed by the metal centres and the bridging-oxygen atoms linking the octahedral units, that have been regarded as a type of macrocyclic bonding system.[5–9] Nomiya and Miwa[5] have proposed a connection between the structural stability of polyoxometalates and the number of closed loops per $MO_6$ octahedron in the form of an index ($\eta$) defined as

$$\eta = \frac{\Sigma BC}{A} \qquad (1)$$

where $A$ is the number of octahedra constituting the polyanion cage, $B$ is the number of $MO_6$ units constituting the closed loop, and $C$ is the number of closed loops (it should be noted that the polyanion cage is not necessarily identical with the whole structure, although it does comprise most of it[5]). A large number of isopoly and heteropoly species have been analyzed,[5–9] and it has been concluded that the structural-stability index can be related to various properties of the polyanion systems. A particularly important observation is that the larger the value of the index, the more a polyoxometalate appears to be stabilized.

Most of the first-principle computational studies of polyoxometalates—at the Hartree–Fock (HF) or density-functional (DF) levels of theory—have been carried out by Bénard, Poblet, and coworkers.[10–19] Many of these calculations have primarily concentrated on the application of molecular electrostatic-potential distributions to understanding the chemical structures and interactions in the polyanion clusters, and have recently been reviewed.[20] Borshch and coworkers have reported DF investigations dealing with electron delocalization[21,22] in substituted isopoly and heteropoly species, and with the reducibility of Keggin anions.[23] In addition to the HF and DF research, some work has been performed using the Xα method.[24–28]

We have recently completed several density-functional investigations of polyoxoanions,[29–31] including the $[M_2O_7]^{2-}$, $[M_4O_{16}]^{8-}$, and $[M_6O_{19}]^{n-}$ clusters formed by Mo and W, and we have also studied $[MO_nCl_{6-n}]^{z-}$ complexes[32] as these are frequently used as simple models for the polymeric systems.[1,2] For example, the $[M_6O_{19}]^{n-}$ anions can be associated with mono-oxo $[MOL_5]$ ("type-I") species. In this article we extend our computational research on polyoxometalates to the $[Mo_7O_{24}]^{6-}$ and $[W_7O_{24}]^{6-}$ anions, which can be (approximately) modelled using *cis* di-oxo $[MO_2L_4]$ ("type-II") species.

The molecular structures of $[Mo_7O_{24}]^{6-}$ and $[W_7O_{24}]^{6-}$ have been fully optimized, and a description of chemical bonding in terms of molecular-orbital and population analyses is presented. Also, the orbital properties of closed loops and the connection with *cis*-$[MO_2Cl_4]^{2-}$ complexes are explored.

## Computational approach

All density-functional calculations reported in this work were performed with the ADF[33,34] program. Functionals based on the Vosko–Wilk–Nusair[35] (VWN) form of the Local Density Approximation[36] (LDA), and on a combination (labelled BP86) of Becke's 1988 exchange[37] and Perdew's 1986 correlation[38] corrections to the LDA were employed. Slater-type-orbital (STO) basis sets of triple-ζ quality incorporating frozen cores and the ZORA relativistic approach (ADF: O 1s, Mo 3d, and W 4f type IV)[33,34] were utilized.

The functional and basis-set choices were based on the results of tests performed on several $[MO_4]$ and $[M_2O_7]$ species.[29,39] Geometry optimizations were carried out using LDA methods, whereas data on thermochemistry and ener-

 DOI: 10.1039/b111221j

getics were extracted from single-point BP86 calculations. Bond and valency indexes were obtained according to the definitions proposed by Mayer[40,41] and by Evarestov and Veryazov,[42] with a program[43] designed for their calculation from the ADF output file. Graphics of molecular orbitals were generated with the MOLEKEL[44] program.

## Results and discussion

### Molecular and electronic structures

**Geometrical properties.** A structural scheme showing atom labels is presented in Fig. 1. There are three different metal

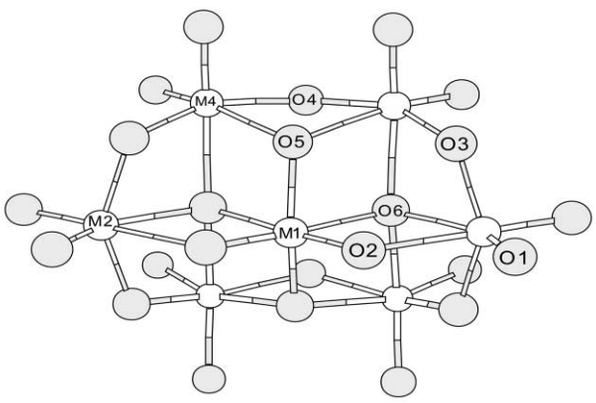


**Fig. 1** Structure and atom labeling scheme for $[M_7O_{24}]^{6-}$ anions.

centres, described as M1, M2, and M4, and four groups of oxygen sites, terminal ($O_t$: O1), two-coordinate ($O_{2c}$: O2, O3, O4), three-coordinate ($O_{3c}$: O5), and four-coordinate ($O_{4c}$: O6) atoms.

Calculated M–O bond distances are given in Table 1, where they are compared with experimental results—taken from the compilations of Tytko *et al.*[45] ($[Mo_7O_{24}]^{6-}$), and from the structural analysis by Ikenoue *et al.*[46] ($[W_7O_{24}]^{6-}$)—that represent $C_{2v}$-symmetry averages of bond-length values observed in crystalline phases. The present calculations correspond to isolated gas-phase molecules, and are thus not directly comparable to solid-state data. Nevertheless, the computational-experimental agreement is, in general, satisfactory. The largest deviations occur in bonds to the $O_t$ and O2 atoms. Although the latter are formally two-coordinate sites, they have also been described as pseudo-terminal ($O_{pt}$) atoms,[45] because the M1–$O_{pt}$ distances are closer to M–$O_t$ than M–$O_{2c}$ bond lengths.

**Table 1** Optimized M–O distances (in pm). Experimental results are given in parentheses

| Parameter | | $[Mo_7O_{24}]^{6-}$ | | $[W_7O_{24}]^{6-}$ | |
|---|---|---|---|---|---|
| M–$O_t$ | M–O1 | 176 | (172) | 178 | (174) |
| M–$O_{2c}$ | M1–O2 | 178 | (174) | 179 | (177) |
| | M2–O2 | 247 | (252) | 244 | (248) |
| | M2–O3 | 191 | (192) | 193 | (190) |
| | M4–O3 | 200 | (198) | 200 | (198) |
| | M4–O4 | 193 | (193) | 195 | (195) |
| M–$O_{3c}$ | M1–O5 | 189 | (190) | 191 | (189) |
| | M4–O5 | 230 | (227) | 230 | (228) |
| M–$O_{4c}$ | M1–O6 | 230 | (226) | 228 | (226) |
| | M2–O6 | 218 | (216) | 222 | (220) |
| | M4–O6 | 215 | (216) | 220 | (217) |

**Molecular-orbital diagrams.** Eigenvalue diagrams for the occupied valence levels of the Mo and W anions are shown in Fig. 2, and the predominant metal and oxygen contributions to the valence orbitals are shown in Fig. 3. The latter are entirely qualitative schemes, and no accurate quantitative correlation

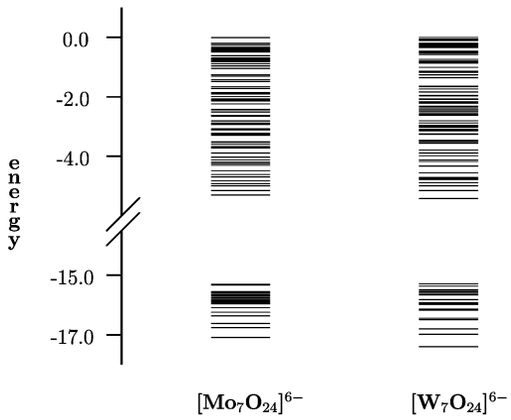


**Fig. 2** Eigenvalue (in eV) diagram for the occupied valence levels (the highest-occupied level is used as reference).

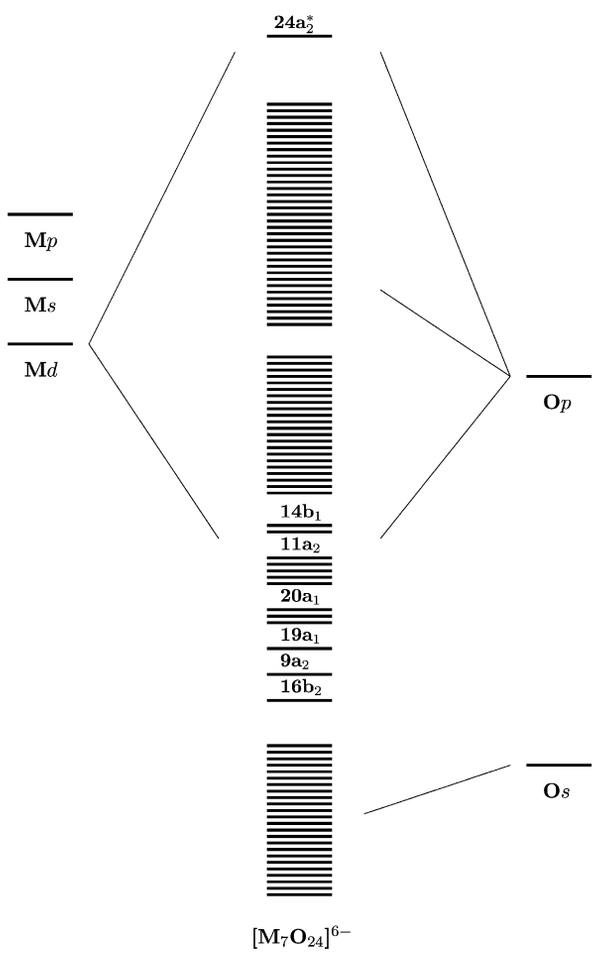


**Fig. 3** Qualitative molecular-orbital diagram showing predominant metal and oxygen contributions to the occupied and lowest virtual valence levels.

exists amongst the positions of the atomic and molecular energy levels. They are intended to summarize the most general and representative characteristics of the electronic structure of the anions, by highlighting the major atomic contributions to the molecular orbitals.

The electronic structures of the Mo and W $[M_7O_{24}]^{6-}$ clusters exhibit similar general characteristics to those of recently studied isopolyanions.[29–31] Three bands comprising two different sets of molecular energy levels, separated by a gap of approximately 10 eV, are observed. The orbitals in the low-lying set are predominantly of Os character and nonbonding. Two overlapping bands can be distinguished in the high-lying set.

Most higher-energy levels correspond to nonbonding combinations of O p-type functions, whereas most lower-energy levels are composed of orbitals incorporating significant contributions from both the metal and oxygen atoms, and represent M–O bonding interactions that are largely M d–O p in character.

**Lowest-unoccupied levels.** An important structural property of the $[M_7O_{24}]^{6-}$ clusters is the fact that all the metal atoms are bonded to two terminal-oxygen sites, and therefore belong to type-II category in Pope's classification scheme.[1] The redox behaviour of type-II systems, unlike that of type-I species (polyanions containing one $M–O_t$ bond per metal atom), is relatively limited, as electron-transfer processes in these species are normally irreversible and difficult.[2]

The redox properties of type-II systems have been frequently interpreted using *cis*-$[MO_2L_4]$ complexes as models for the individual $MO_6$ units in the polyanions.[1,2,47] The M–O antibonding nature of the lowest-unoccupied level (LUMO) in the oxidized *cis* di-oxo species has been associated with the observed difficulties in the reduction of type-II polyoxometalates.

Recent calculations[32] have revealed that the LUMOs of Mo and W *cis*-$[MO_2Cl_4]^{2-}$ complexes correspond to π-like antibonding interactions between M $d_{xz}$ and O $p_x$ orbitals (Fig. 4).

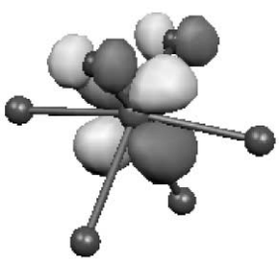

**Fig. 4** Spatial representation of the LUMO ($7b_1$ orbital) in *cis*-$[MO_2Cl_4]^{2-}$ complexes.

The present results indicate that the LUMO in the $[M_7O_{24}]^{6-}$ anions is the $24a_2$ level (Fig. 3). A spatial plot is given in Fig. 5, and shows that, as in the model complexes, this orbital can be characterized as an interaction of π-antibonding nature between metal and terminal-oxygen atoms. In addition to the first vacant level, the next four LUMOs are predominantly M d–O p and π-antibonding in character, and involve the M2, M4, $O_t$, and also the M1 and $O_{pt}$ atoms.

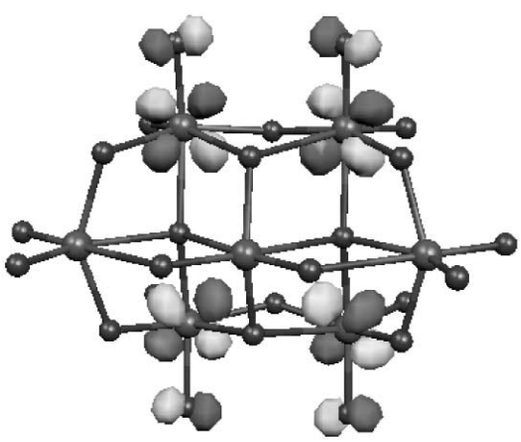

**Fig. 5** Spatial representation of the LUMO ($24a_2$ orbital) in $[M_7O_{24}]^{6-}$ anions.

**Bridging bonds and closed loops.** It has been pointed in the 'Introduction' that Nomiya and Miwa have developed the idea—and quantified it through the index defined by eqn. (1)—of the importance of metal–oxygen interactions along closed loops as a structural-stability factor in polyoxometalates. These authors have also suggested that both σ and π bonding between the metal and bridging-oxygen ($O_b$) atoms should be involved.[5] The orbital properties of the closed loops are of particular interest as these structures have sometimes been described as analogous to conjugated bonds in typical aromatic systems.[28,47]

In the $[M_7O_{24}]^{6-}$ clusters, one $[M_6O_6]$ closed loop has been considered.[5] This structure involves the M2 and M4 centres and the two-coordinate O3 and O4 oxygen sites. The $16b_2$ molecular orbital is a suitable example as it is a combination of M2 and M4 $d_{z^2}$-type functions with O3 and O4 p-type functions (the contribution from the M1 and remaining O atoms are small or negligible). Its spatial representation is given in Fig. 6 (part a),

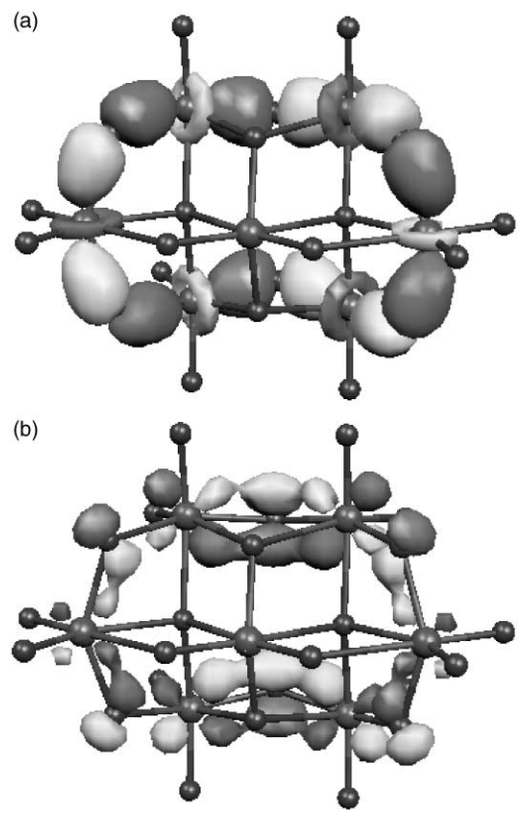


**Fig. 6** Spatial representation of (a) σ ($16b_2$ orbital) and (b) π ($14b_1$ orbital) $[M_6O_6]$ closed loops.

and can be described as a σ-like interaction along the $[M_6O_6]$ ring. Analogous π-like closed loops are also observed, an example being shown in Fig. 6 (part b), where the contributions from the M2, M4, O3, and O4 atoms in the $14b_1$ orbital are plotted.

Nomiya and Miwa have apparently ruled out the possible participation in closed loops of oxygen atoms in *trans* configuration with respect to terminal bonds.[5] This argument seems to be based on the fact that individual *trans*-to-oxo bonds in polyanions are rather weak. However, in the $[M_7O_{24}]^{6-}$ anions it is possible to describe closed loops that involve oxygen atoms participating in *trans*-to-oxo bonds. Examples are given in Fig. 7, where the σ and π ($9a_2$ and $19a_1$ orbitals, respectively) components of an $[M_4O_4]$ ring formed by interconnecting M4–O6–M4 and M4–O4–M4 bridges are displayed. In this case, four $M–O_{4c}$ bonds that lie *trans* to terminal $M4–O_t$ groups are incorporated into a closed loop. There are also a number of orbitals that contain the *trans*-to-oxo $M–O_{3c}$ (M4–O5) bonds in rings of variable size and composition.

The $M1–O_{3c}$ bonds are structurally similar to the $M–O_{2c}$ bonds (M–O distances are comparable, and the configurations are *cis* to terminal or pseudo-terminal oxygen atoms), and there is also a resemblance on the molecular-orbital level. The spatial plots of the $20a_1$ and $11a_2$ orbitals given in Fig. 8 (only

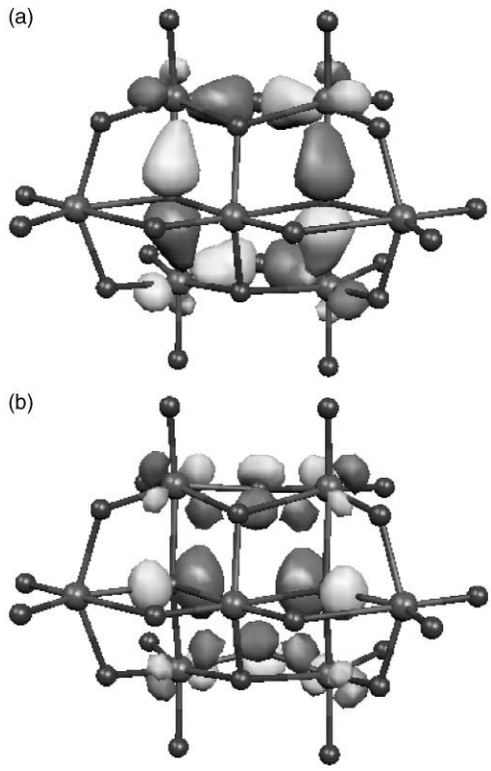


**Fig. 7** Spatial representation of (a) σ ($9a_2$ orbital) and (b) π ($19a_1$ orbital) $[M_4O_4]$ closed loops.

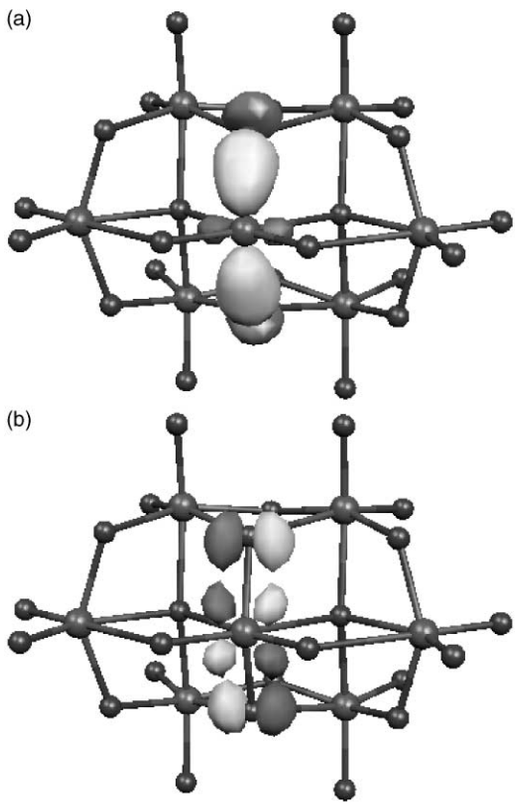


**Fig. 8** Spatial representation of (a) σ ($20a_1$ orbital) and (b) π ($11a_2$ orbital) [O5–M1–O5] bonding.

the density at the M1 and O5 atoms is displayed) show that the M1–$O_{3c}$ interactions can be described as multicentred σ and π bonds but, unlike the M–$O_{2c}$ interactions, the electron delocalization cannot extend over a ring of metal and equivalent oxygen sites.

The present results support the idea that electron delocalization that involves M–$O_b$ σ and π bonds interconnected along $[M_nO_n]$ closed loops plays a role in the chemical bonding in $[M_7O_{24}]^{6-}$ anions, but the general nature of the electronic structures does not suggest that this phenomenon should stand out as a stabilizing factor. The structural stability derived from the orbital interactions appears to be the result of the combined effect of all bonding modes involving the various oxygen types.

**Table 2** Mulliken charges for metal and oxygen atoms

| Atom | $[Mo_7O_{24}]^{6-}$ | $[W_7O_{24}]^{6-}$ |
|---|---|---|
| M1 | 2.16 | 2.29 |
| M2 | 1.91 | 2.07 |
| M4 | 2.06 | 2.20 |
| $O_t$ | −0.77 | −0.82 |
| $O_{pt}$ | −0.80 | −0.83 |
| $O_{2c}$ | −0.89 | −0.93 |
| $O_{3c}$ | −0.95 | −0.98 |
| $O_{4c}$ | −1.11 | −1.12 |

**Table 3** Populations of metal basis functions, given as percentage per individual orbital

| Molecule | Atom | s | p | d |
|---|---|---|---|---|
| $[Mo_7O_{24}]^{6-}$ | M1 | 0.0 | 1.4 | 19.2 |
| | M2 | 0.2 | 1.2 | 19.2 |
| | M4 | 0.0 | 1.1 | 19.3 |
| $[W_7O_{24}]^{6-}$ | M1 | 4.1 | 1.4 | 18.4 |
| | M2 | 5.1 | 1.3 | 18.2 |
| | M4 | 4.7 | 1.2 | 18.3 |

## Population methods

The results presented in this section are based on Mulliken and Mayer methodology. These methods are known to exhibit basis-set dependence, but (relative) Mulliken charges and Mayer bond indexes can nonetheless provide valuable chemical information for inorganic systems, if uniformity and consistency of the basis sets are maintained.[48] Furthermore, Mulliken analysis has been described as "not an arbitrary choice . . . but consistent with the internal structure of the molecular-orbital formalism".[40]

**Mulliken analysis.** Mulliken charges for all atoms and metal basis-function populations are given in Tables 2 and 3. The results for the metal atoms correspond to $d^4$ electronic configurations, in contrast to the formal $d^0$ assignment; and the charges are considerably smaller than the formal oxidation states. The s and p orbitals are sparingly populated, in accordance with the molecular-orbital analysis indicating predominant participation of M d functions in M–O bonding. The slightly higher s and lower d characters of W configurations are probably related to the stronger relativistic effects that are characteristic of the 5d elements.[49]

The negative charge is distributed over all types of oxygen atoms, and the individual values are relatively close to one another, although an increasing trend with the coordination number is observed. It is also interesting to note that the terminal and pseudo-terminal sites are significantly charged, and collectively bear a slightly higher proportion of the total negative charge than the bridging atoms do.

**Mayer analysis.** Mayer bond-order indexes are given in Table 4. Also included are the results obtained with a bond-valence model based on the following relationship[45]

$$\log s = \frac{(d_0 - d)}{B} \qquad (2)$$

**Table 4** Mayer indexes for M–O bonds. Results from classical bond-valence analysis are given in parentheses

| Bond | $[Mo_7O_{24}]^{6-}$ | | $[W_7O_{24}]^{6-}$ | |
|---|---|---|---|---|
| M1–$O_{pt}$ | 1.35 | (1.39) | 1.39 | (1.36) |
| M1–$O_{3c}$ | 0.83 | (1.06) | 0.85 | (1.01) |
| M1–$O_{4c}$ | 0.22 | (0.39) | 0.25 | (0.41) |
| M2–$O_t$ | 1.54 | (1.42) | 1.57 | (1.37) |
| M2–$O_{pt}$ | 0.26 | (0.26) | 0.23 | (0.28) |
| M2–$O_{2c}$ | 0.82 | (1.01) | 0.82 | (0.97) |
| M2–$O_{4c}$ | 0.34 | (0.53) | 0.35 | (0.48) |
| M4–$O_t$ | 1.59 | (1.47) | 1.62 | (1.40) |
| M4–$O_{2c}$ | 0.67 | (0.89) | 0.70 | (0.88) |
| M4–$O_{3c}$ | 0.28 | (0.39) | 0.27 | (0.39) |
| M4–$O_{4c}$ | 0.30 | (0.57) | 0.30 | (0.50) |

where $s$ is the bond valence, $d_0$ is the single-bond length, $B$ defines the slope of the bond length–bond valence functions, and $d$ is a calculated bond distance. The computational indexes compare well with the bond-valence values, the deviations falling within a range of 0.2–0.3 units.

In general, the relative values of the Mayer index for the different bonds follow the trend that would be predicted by a comparison of the corresponding M–O distances. There are also some particular results than can be analyzed in more detail. Interactions involving $O_{2c}$ and $O_{3c}$ atoms (M1–O5, M2–O3, M4–O4 bonds) display a typical multiple molecular-orbital structure (Figs. 6 and 8), but exhibit approximately single character. The interactions between M4 and $O_{4c}$ atoms (M4–O6 bonds) also have σ and π properties (Fig. 7) but the corresponding bond orders are rather small. These results reflect the effects of the extensive delocalization of the electron density (along the $[M_nO_n]$ closed loops in particular, and over the whole molecule in general) on the properties of the individual bonds. Fractional multiple character is found for the terminal bonds, and the index is significantly smaller than the maximum possible covalency for the $MO_2$ fragment, in accord with ionic contributions being an important factor in M–$O_t$ interactions.

The structural and charge analyses have indicated that the $O_{pt}$ atoms, despite being formally two-coordinate, behave as terminal sites. The Mayer index shows some degree of multiple M–$O_{pt}$ bonding, but of smaller magnitude than that of M–$O_t$ interactions, and suggests that although $O_{pt}$ and $O_t$ atoms are closely related, their bonding properties do not appear to be exactly equivalent (this result is not obtained with the bond-valence model because, unlike Mayer analysis, the former directly reflects M–O distances, not the nature of orbital interactions). These observations are consistent with the fact that the second bond involving the pseudo-terminal atoms (M2–$O_{pt}$) is weak but not of negligibly low order.

**Oxygen valency.** Covalency and full-valency indexes for the oxygen atoms are shown in Table 5. The former are calculated as a sum of all Mayer indexes for a particular atom (and therefore include some contributions—for example O–O interactions—that may be small but not necessarily negligible), whereas the latter are a combined measure of covalent (covalency) and ionic (electrovalency) bonding based on Mayer and Mulliken results.

An interesting structural feature of polyoxoanions is the presence of noticeably long M–O bonds in *trans* configuration with respect to terminal groups. This phenomenon has been normally described as a manifestation of the strong *trans* influence of the multiply-bonded oxo sites,[2] and in the $[M_7O_{24}]^{6-}$ anions it is observed in the bonding to $O_{pt}$ and $O_{3c}$ atoms, the (*trans*-to-oxo) M2–$O_{pt}$ and M4–$O_{3c}$ distances being much longer, respectively, than the Ml–$O_{pt}$ and M1–$O_{3c}$ bond lengths.

**Table 5** Covalency and full-valency indexes for oxygen atoms

| Molecule | Atom | Covalency | Full valency |
|---|---|---|---|
| $[Mo_7O_{24}]^{6-}$ | $O_t$ | 1.99 | 2.25 |
| | $O_{pt}$ | 1.96 | 2.25 |
| | $O_{2c}$ | 1.85 | 2.20 |
| | $O_{3c}$ | 1.76 | 2.17 |
| | $O_{4c}$ | 1.52 | 2.11 |
| $[W_7O_{24}]^{6-}$ | $O_t$ | 1.94 | 2.24 |
| | $O_{pt}$ | 1.92 | 2.23 |
| | $O_{2c}$ | 1.80 | 2.19 |
| | $O_{3c}$ | 1.70 | 2.15 |
| | $O_{4c}$ | 1.48 | 2.08 |

The covalency indexes for the bridging ($O_{2c}$, $O_{3c}$, $O_{4c}$) sites display some correlation with *trans*-influence effects, for example, the values are lower for $O_{4c}$ atoms, where all bonds are *trans* to terminal or pseudo-terminal groups, than for $O_{2c}$ atoms, where no *trans*-to-oxo bonds are found. Nevertheless, the differences in total covalency are considerably smaller than those observed for the individual bond orders. Furthermore, the full-valency results suggest that, despite the variety of bond lengths and coordination environments, the overall bonding capacities of the various oxygen atoms are similar.

The $O_{pt}$ atoms can compensate for the weak (*trans*-to-oxo) M2–$O_{pt}$ bond *via* the strong pseudo-terminal (M1–$O_{pt}$) interaction, whereas the $O_{4c}$ atoms can overcome the unfavourable *trans*-influence effects by adopting a high-coordination environment. The $O_{3c}$ atoms utilize a combination of both mechanisms, as they are relatively high-coordinate sites and also form a moderately strong bond in *cis*-to-oxo configuration.

Although the methodology is not directly related, the population results are comparable, on a qualitative basis, to the observations made by Tytko *et al*. in their bond-valence analysis of polyoxometalates.[45,50] These authors have considered that the acceptance of negative charge by $O_t$ and $O_{pt}$ sites and the non-maximization of M–$O_t$ covalency should play an important role in polyoxometalate structures, and have pointed out that oxygen atoms involved in (individually) weak *trans*-to-oxo bonds can nonetheless be strongly bound overall.

## Conclusion

The molecular and electronic structures of the $[Mo_7O_{24}]^{6-}$ and $[W_7O_{24}]^{6-}$ isopolyanions have been calculated using density-functional theory. The structural and bonding properties are in good agreement with experimental data and bond-valence descriptions for these species.

The molecular-orbital and population analyses have indicated that M–O bonding is largely M d–O p in character. Multicentred bridging interactions of σ and π nature have been observed and, in particular, those involving the two-coordinate oxygen atoms exhibit a closed-loop delocalization pattern along a twelve-membered [M–$O_{2c}$] ring, as originally proposed by Nomiya and Miwa. However, it has been found that bonding involving all types of bridging sites, not only the $O_{2c}$, atoms, can be described in terms of orbital rings.

The population results have satisfactorily reproduced observations based on bond-valence models. The valency analyses have revealed similarities in the overall bonding capacity of the various oxygen sites. Fractional (not maximized) multiple character has been obtained for terminal and pseudo-terminal bonds. The molecular-orbital structure of bonds in *cis*-to-oxo configuration is typical of a multiple σ–π interaction, but the Mayer indexes correspond to approximately single character. Bonds in *trans*-to-oxo configuration are of considerably low order, although some interactions also exhibit multiple character. The Mulliken analysis has yielded a distribution of the negative charge over all types of oxygen

sites, and metal charges and orbital populations that are significantly different from the formal oxidation states and electronic configurations.

## Acknowledgements

The authors would like to thank EPSRC, the Cambridge Overseas Trust, Selwyn College (Cambridge), and the University of Hull for financial support, and the Computational Chemistry Working Party for access to computational facilities in the Rutherford Appleton Laboratory.

## References

1 M. T. Pope, *Heteropoly and Isopoly Oxometalates*, Springer-Verlag, Heidelberg, 1983.
2 M. T. Pope and A. Müller, *Angew. Chem., Int. Ed. Eng.*, 1991, **30**, 34.
3 L. C. W. Baker and D. C. Glick, *Chem. Rev.*, 1998, **98**, 3.
4 M. T. Pope, A. Müller, editors, *Polyoxometalates: from Platonic Solids to Anti-retroviral Activity*, Kluwer, Dordrecht, 1994.
5 K. Nomiya and M. Miwa, *Polyhedron*, 1984, **3**, 341.
6 K. Nomiya and M. Miwa, *Polyhedron*, 1985, **4**, 89.
7 K. Nomiya and M. Miwa, *Polyhedron*, 1985, **4**, 675.
8 K. Nomiya and M. Miwa, *Polyhedron*, 1985, **4**, 1407.
9 K. Nomiya, *Polyhedron*, 1987, **6**, 309.
10 M.-M. Rohmer, R. Ernenwein, M. Ulmschneider, R. Wiest and M. Bénard, *Int. J. Quantum Chem.*, 1991, **40**, 723.
11 J.-Y. Kempf, M.-M. Rohmer, J.-M. Poblet, C. Bo and M. Bénard, *J. Am. Chem. Soc.*, 1992, **114**, 1136.
12 M.-M. Rohmer and M. Bénard, *J. Am. Chem. Soc.*, 1994, **116**, 6959.
13 J. Devémy, M.-M. Rohmer, M. Bénard and R. Ernenwein, *Int. J. Quantum Chem.*, 1996, **58**, 267.
14 M.-M. Rohmer, J. Devémy, R. Wiest and M. Bénard, *J. Am. Chem. Soc.*, 1996, **118**, 13007.
15 J. M. Maestre, J. P. Sarasa, C. Bo and J. M. Poblet, *Inorg. Chem.*, 1998, **37**, 3071.
16 J. M. Maestre, J. M. Poblet, C. Bo, N. Casañ-Pastor and P. Gomez-Romero, *Inorg. Chem.*, 1998, **37**, 3444.
17 A. Dolbecq, A. Guirauden, M. Fourmigué, K. Boubekeur, P. Batail, M.-M. Rohmer, M. Bénard, C. Coulon, M. Sallé and P. Blanchard, *J. Chem. Soc., Dalton Trans.*, 1999, 1241.
18 J. M. Maestre, X. López, C. Bo, J. M. Poblet and N. Casañ-Pastor, *J. Am. Chem. Soc.*, 2001, **123**, 3749.
19 X. López, J. M. Maestre, C. Bo and J. M. Poblet, *J. Am. Chem. Soc.*, 2001, **123**, 9571.
20 M.-M. Rohmer, M. Bénard, J.-P. Blaudeau, J.-M. Maestre and J.-M. Poblet, *Coord. Chem. Rev.*, 1998, **178–180**, 1019.
21 H. Duclusaud and S. A. Borshch, *Inorg. Chem.*, 1999, **38**, 3489.
22 H. Duclusaud and S. A. Borshch, *J. Am. Chem. Soc.*, 2001, **123**, 2825.
23 S. A. Borshch, H. Duclusaud and J. M. M. Millet, *Appl. Catal. A*, 2000, **200**, 103.
24 K. Eguchi, T. Seiyama, N. Yamazoe, S. Katsuki and H. Taketa, *J. Catal.*, 1988, **111**, 336.
25 H. Taketa, S. Katsuki, K. Eguchi, T. Seiyama and N. Yamazoe, *J. Phys. Chem.*, 1986, **90**, 2959.
26 S. X. Xiao, J. Ji, T. L. Chen, T. X. Cai and G. S. Yan, *THEOCHEM*, 1990, **63**, 33.
27 T. L. Chen, J. Ji, S. X. Xiao, T. X. Cai and G. S. Yan, *Int. J. Quantum Chem.*, 1992, **44**, 1015.
28 T. Cai, Z. D. Chen, X. Z. Wang, L. M. Li and J. X. Lu, *Prog. Nat. Sci.*, 1997, **7**, 554.
29 A. J. Bridgeman and G. Cavigliasso, *J. Phys. Chem. A*, 2001, **105**, 7111.
30 A. J. Bridgeman and G. Cavigliasso, *Polyhedron*, 2001, **20**, 3101.
31 A. J. Bridgeman and G. Cavigliasso, *Inorg. Chem.*, 2002, **41**, 1761.
32 A. J. Bridgeman and G. Cavigliasso, *J. Chem. Soc., Dalton Trans.*, 2001, 3556.
33 ADF2000.02: E. J. Baerends, D. E. Ellis and P. Ros, *Chem. Phys.*, 1973, **2**, 41; L. Versluis and T. Ziegler, *J. Chem. Phys.*, 1988, **322**, 88; G. te Velde and E. J. Baerends, *J. Comput. Phys.*, 1992, **99**, 84; G. Fonseca Guerra, J. G. Snijders, G. te Velde and E. J. Baerends, *Theor. Chem. Acc.*, 1998, **99**, 391.
34 G. te Velde, F. M. Bickelhaupt, E. J. Baerends, C. Fonseca Guerra, S. J. A. van Gisbergen, J. G. Snijders and T. Ziegler, *J. Comput. Chem.*, 2001, **22**, 931.
35 S. H. Vosko, L. Wilk and M. Nusair, *Can. J. Phys.*, 1980, **58**, 1200.
36 W. Kohn and L. J. Sham, *Phys. Rev. A*, 1965, **140**, 1133.
37 A. D. Becke, *Phys. Rev. A: At. Mol. Opt. Phys.*, 1988, **38**, 3098.
38 J. P. Perdew, *Phys. Rev. B: Condens. Matter*, 1986, **33**, 8822.
39 A. J. Bridgeman and G. Cavigliasso, *Polyhedron*, 2001, **20**, 2269.
40 I. Mayer, *Chem. Phys. Lett.*, 1983, **97**, 270.
41 I. Mayer, *Int. J. Quantum Chem.*, 1984, **26**, 151.
42 R. A. Evarestov and V. A. Veryazov, *Theor. Chim. Acta*, 1991, **81**, 95.
43 MAYER. A program to calculate Mayer bond-order indexes from the output of the electronic structure packages GAMESS-UK, GAUSSIAN, and ADF, written by A. J. Bridgeman, University of Hull (2001). Available from the author on request.
44 MOLEKEL: An Interactive Molecular Graphics Tool. S. Portmann and H. P. Lüthi, *CHIMIA*, 2000, **54**, 766.
45 K. H. Tytko, J. Mehmke and S. Fischer, *Struct. Bonding (Berlin)*, 1999, **93**, 129.
46 K. Ikenoue, M. Mikuriya, O. Miyauchi, R. Nukada and A. Yagasaki, *Bull. Chem. Soc. Jpn.*, 1994, **67**, 2590.
47 R. B. King, *Inorg. Chem.*, 1991, **30**, 4437.
48 A. J. Bridgeman, G. Cavigliasso, L. R. Ireland and J. Rothery, *J. Chem. Soc., Dalton Trans.*, 2001, 2095.
49 N. Kaltsoyannis, *J. Chem. Soc., Dalton Trans.*, 1997, 1.
50 K. H. Tytko, *Struct. Bonding (Berlin)*, 1999, **93**, 67.